Transactions of the Materials Research Society of Japan 27 [1] 7-12 (2002)

Local atomic structures in (Fe, Co)-Nd-B and Fe-Nb-B glassy alloys studied by X-ray diffraction

Muneyuki Imafuku [a*], Wei Zhang [a] and Akihisa Inoue [b]
[a] Inoue Superliquid Glass Project, ERATO, JST, Sendai 982-0807, Japan
[b] Institute for Materials Research, Tohoku University, Sendai 980-8577, Japan
*Present address: Advanced Technology Research Laboratories, Nippon Steel Corporation, Futtsu, 293-8511, Japan
e-mail: crystal@re.nsc.co.jp

Variation in the local atomic structures in (Fe, Co)-Ln-B (Ln=Nd) and Fe-M-B (M=Nb) glassy alloys was investigated in wide composition ranges of boron by the X-ray diffraction method. Distorted dense random network of trigonal prism-like local ordering structure around boron was identified in both alloys within the glassy composition region. In this network structure, Nd atoms are located between the prisms and Nb atoms are on the vertex site of the prisms, respectively. It is suggested that the strong chemical affinities of Nd-B or Nb-B and Nb-Fe pairs with large atomic differences between the constituents contribute to the strengthening of the network of the prisms so as to suppress the rearrangement of the constituent elements on a long-range scale in these alloys.
Keywords: iron-base glassy alloys, iron-niobium-boron, iron-neodymium-boron, x-ray diffraction, local atomic structure

1. Introduction

Recent findings of ferrous glassy alloys with a large glass-forming ability enable us to synthesize the bulk-formed soft magnetic materials. For example, by adding transition metal in Fe-B based system, (Fe, Co)-(Zr, Hf, Nb)-B [1] and (Fe, Co)-(Zr, Nb, Ta)-(Mo, W)-B [2] glassy alloys have been synthesized in a thick sheet with thickness up to 5 mm. These alloys satisfy Inoue's three empirical rules [3-5] for the achievement of high glass-forming ability, *i.e.*, (1) the multicomponet system consisting of more than three elements, (2) the different atomic size ratios beyond about 12 % among the main components, (3) the negative heats of mixing among their elements. According to these rules, a new series of glassy Fe-Co-(Nd, Sm, Tb, Dy, Pr)-B alloys exhibiting glass transition and supercooled liquid state before crystallization was found by Zhang *et.al* [6-8]. In their glassy alloys with these rules, the existence of a kind of unique local atomic structure leading to the suppression of the nucleation and crystal growth upon heating has been thought. Actually, a trigonal prism-like local atomic structure has been reported in glassy Fe-Co-(Sm, Tb, Dy)-B and Fe-(Zr, Hf, Nb)-B alloys [9,10]. However, there is no systematic study on the variation of the local atomic structures with their boron concentration. In this paper, we intend to present the dependence of boron concentration on the thermal stability and the local atomic structure of typical Fe-Ln-B and Fe-TM-B glassy alloys and to discuss the origin for high thermal stability of these alloys.

2. Experimental

Two series of glassy alloys, $Fe_{87-x}Co_{10}Ln_3B_x$ (Ln=Nd, x=16, 18, 20, 22, 26,30, 35 or 40) and $Fe_{90-x}TM_{10}B_x$ (TM=Nb, x=10, 20 or 30), were prepared by single-roller melt spinning technique in an argon atmosphere from the master ingots of their nominal compositions. Thermal stability was examined by differential scanning calorimetry (DSC) at a heating rate of 0.67 K/s. Densities of the samples were measured by Archimedean method with toluene [11] for the X-ray diffraction analysis.

The ordinary X-ray diffraction measurements were carried out by using monochromatic Mo K_α radiation in order to obtain the local atomic structures of $Fe_{87-x}Co_{10}Nd_3B_x$ (x=16, 26, 35 or 40) alloys. The maximum Q–value ($Q = 4\pi\sin\theta/\lambda$) of the present study was 150 nm^{-1}, which is considered to be large enough not to give serious truncating effect in Fourier transformation [12]. Scattered intensities were corrected for air scattering, absorption and polarization, and then converted to electron units per atom with the generalized Krogh-Moe-Norman method [12] using the X-ray scattering factors and the theoretical Compton scattering intensity.

The anomalous X-ray scattering (AXS) measurements near the energy of Nb K absorption edge

($E_{abs,Nb\ K}$ = 18.9896 KeV) were carried out in the case of $Fe_{90-x}Nb_{10}B_x$ (x=10,20 or 30) alloys at the beam line BL-7C in the Photon Factory of the National Laboratory for High Energy Accelerator Research Organization, Tsukuba, Japan. Two incident X-ray energies at 30 and 300 eV below $E_{abs,Nb\ K}$ were selected in order to gain a large difference in the anomalous dispersion term for Nb, f'_{Nb}. The ordinary intensity profiles were analyzed by using the data at 300 eV below $E_{abs,Nb\ K}$. The obtained differential intensity profiles were corrected and converted to electron units per atom with the same way as the ordinary X-ray diffraction analysis.

The ordinary or differential interference functions were Fourier transformed to obtain the total or environmental radial distribution functions. The least-squares calculation of Narten and Levy formula [13,14] for the interference function was used to determine the structural parameters of coordination numbers (N) and interatomic distances (r) for the neighboring pairs. The details of the data processing have been already explained in previous papers [10, 12, 15].

3. Results and discussion

Figures 1 and 2 show the DSC curves for the $Fe_{87-x}Co_{10}Nd_3B_x$ (x=16, 18, 20, 22, 26,30, 35 or 40) and $Fe_{90-x}Nb_{10}B_x$ (x=10,20 or 30) alloys. Although the amorphous alloys were obtained over the whole composition range, the glass transition followed by the appearance of supercooled liquid region is seen in the composition range of 18 to 30 at.% boron for $Fe_{87-x}Co_{10}Nd_3B_x$ and 20 to 30 at.% boron for $Fe_{90-x}Nb_{10}B_x$ alloys. The values of the glass transition temperature (T_g), crystallization temperature (T_x) and ΔT_x ($=T_x - T_g$) are summarized in Table I.

Structural analyses were carried out for the $Fe_{87-x}Co_{10}Nd_3B_x$ (x=16, 26, 35 or 40) and $Fe_{90-x}Nb_{10}B_x$ (x=10,20 or 30) alloys. The observed densities and number densities for the present samples are summarized in Table II. With increasing boron concentration, the density decreases, whereas the number density increases in both alloy series.

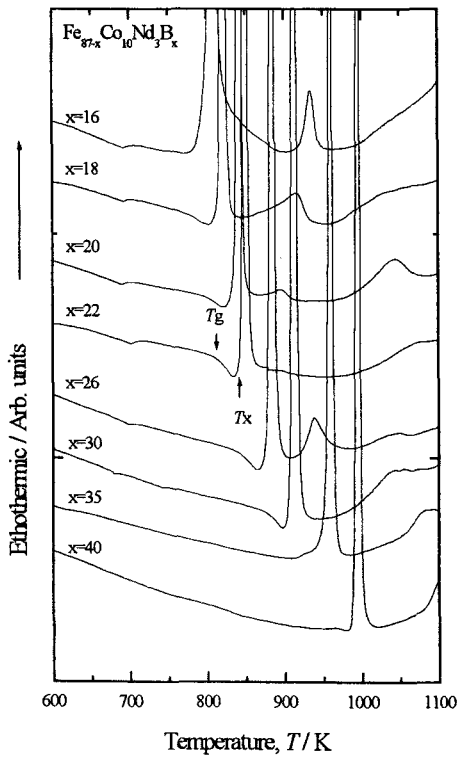

Fig.1 The DSC curves of $Fe_{87-x}Co_{10}Nd_3B_x$ (x=16, 18, 20, 22, 26,30, 35 or 40) glassy alloys.

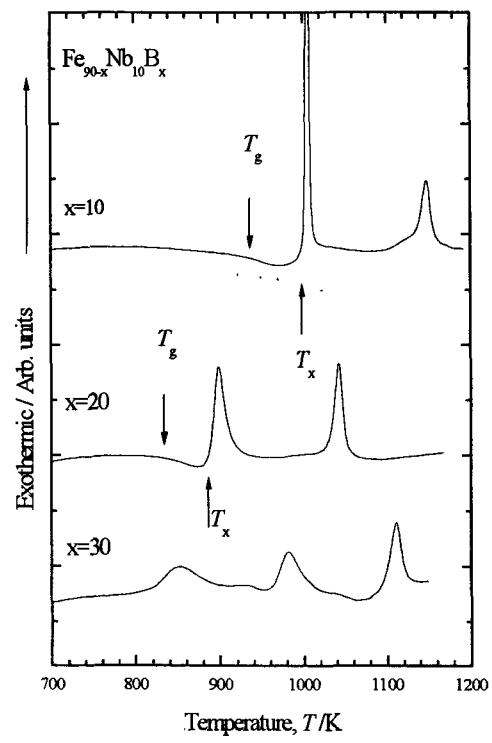

Fig.2 The DSC curves of $Fe_{90-x}Nb_{10}B_x$ (x=10, 20 or 30) glassy alloys.

Table I The values of T_g, T_x and ΔT_x fo the $Fe_{87-x}Co_{10}Nd_3B_x$ (x=16, 18, 20, 22, 26,30, 35 or 40) and $Fe_{90-x}Nb_{10}B_x$ (x=10,20 or 30) alloys.

		T_g (K)	T_x (K)	ΔT_x (K)
$Fe_{87-x}Co_{10}Nd_3B_x$	X=16	---	793	---
	18	780	814	34
	20	798	835	37
	22	811	846	35
	26	843	879	36
	30	878	909	31
	35	---	916	---
	40	---	961	---
$Fe_{90-x}Nb_{10}B_x$	X=10	---	815	---
	20	833	886	53
	30	934	1001	67

Table II The observed densities, ρ and number densities, $\#D$ of $Fe_{87-x}Co_{10}Nd_3B_x$ (x=16, 26, 35, 40) and $Fe_{90-x}Nb_{10}B_x$ (x=10, 20, 30) alloys.

		ρ (Mg/m^3)	$\#D$ ($atoms/nm^3$)
$Fe_{87-x}Co_{10}Nd_3B_x$	X=16	7.70	89.9
	26	7.58	96.9
	35	7.43	103.9
	40	7.24	106.9
$Fe_{90-x}Nb_{10}B_x$	X=10	7.96	87.1
	20	7.68	91.5
	30	7.54	98.6

The ordinary interference functions $Qi(Q)$ of the $Fe_{87-x}Co_{10}Nd_3B_x$ (x=16, 26, 35 or 40) glassy alloys are shown in Fig. 3. The solid and dotted curves are the experimental functions and calculated ones derived from the least-squares fitting analysis, respectively. The total radial distribution functions (RDFs) calculated from the Fourier transformation of the interference functions are shown in Fig. 4. The main possible atomic correlations of B-Fe, Fe-(Fe,Co) and Fe-Nd are indexed in this figure. Similarly, the ordinary and differential interference functions, $Qi(Q)$ and $Q\Delta i_{Nb}(Q)$, of the $Fe_{90-x}Nb_{10}B_x$ (x=10, 20 or 30) glassy alloys are shown in Figs. 5 and 6, respectively. The main periodic features of the experimental curves of $Q\Delta i_{Nb}(Q)$ in Fig. 6 were well reproduced by the fitting calculation with the environmental structural parameters around Nb. The total structural parameters were calculated combining the AXS and the ordinary X-ray analyses. Figure 7 shows the total RDFs of the $Fe_{90-x}Nb_{10}B_x$ (x=10, 20 or 30) glassy alloys. The main possible atomic correlations of B-Fe, Fe-Fe and Nb-Fe are also indexed in this figure.

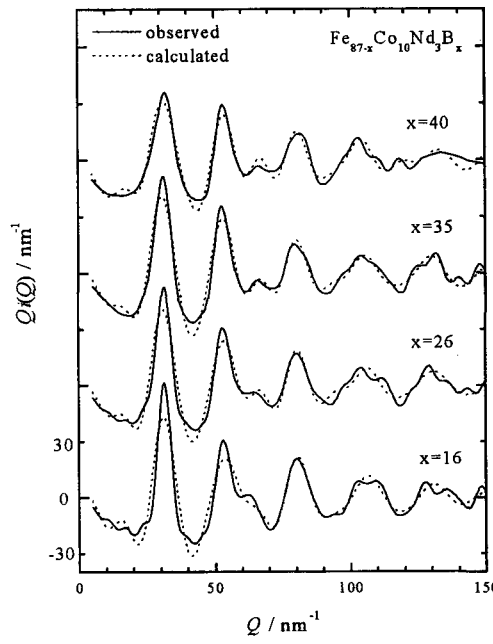

Fig.3 Ordinary interference functions, $Qi(Q)$ in $Fe_{87-x}Co_{10}Nd_3B_x$ (x=16, 26, 35 or 40) glassy alloys. The solid and dotted curves correspond to the experimental and calculated ones.

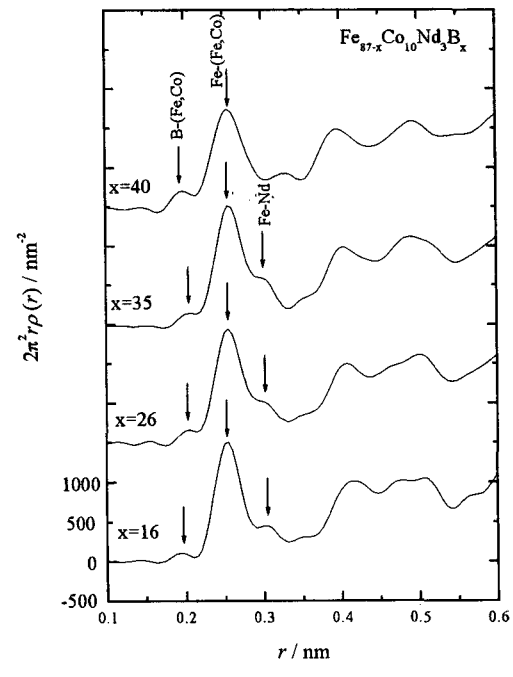

Fig.4 Radial distribution functions (RDFs) of $Fe_{87-x}Co_{10}Nd_3B_x$ (x=16, 26, 35 or 40) glassy alloys. The positions of the atomic correlations of B-(Fe,Co), Fe-(Fe,Co) and Fe-Nd are indicated by arrows.

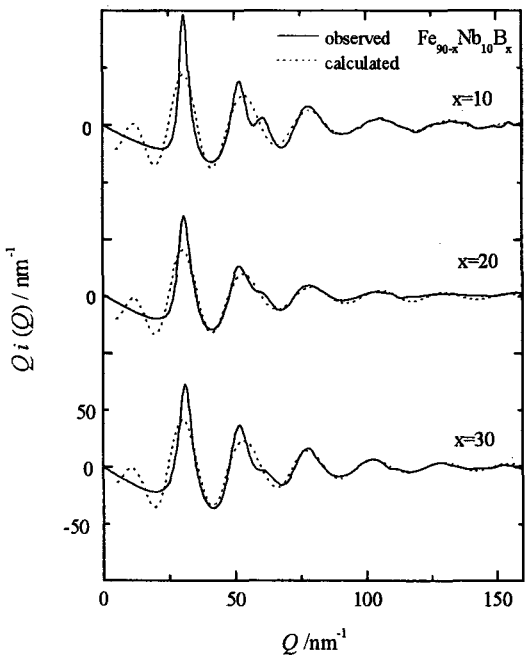

Fig.5 Ordinary interference functions, $Qi(Q)$ in $Fe_{90-x}Nb_{10}B_x$ (x=10, 20 or 30) glassy alloys. The solid and dotted curves correspond to the experimental and calculated ones.

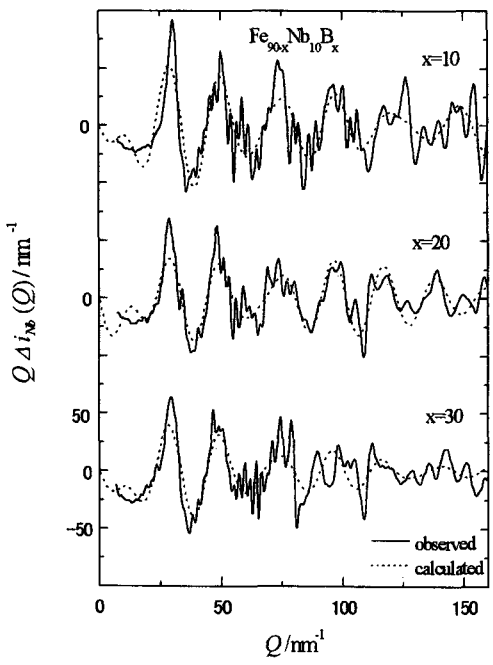

Fig.6 Energy differential interference functions of Nb, $Q\Delta i_{Nb}(Q)$ in amorphous $Fe_{90-x}Nb_{10}B_x$ (x=10, 20 or 30) alloys. The solid and dotted curves correspond to the experimental and calculated ones.

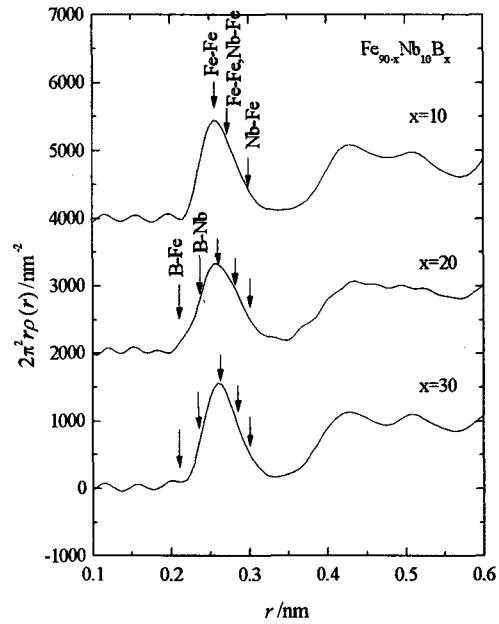

Fig.7 Radial distribution functions (RDFs) of $Fe_{90-x}Nb_{10}B_x$ (x=10, 20 or 30) glassy alloys. The positions of the atomic correlations of B-Fe, B-Nb, Fe-Fe and Nb-Fe are indicated by arrows.

In transition metal-metalloid amorphous alloys, especially in Fe-B system, amorphous structures can be classified into two types, *i.e.* the Bernal type and chemical order type by their composition [16]. When boron content is larger than 18 at.% in Fe-B system, a kind of chemical ordering structure around boron becomes dominant and the stereo-chemical model with the random network of the trigonal prism unit of Fe_3B has been identified [17]. With the analogy of the classical amorphous Fe-B alloys, we intend to characterize the present alloys by the fitted structural parameters, especially the coordination number of metals around boron.

Figure 8 shows the coordination numbers of first nearest neighboring B-(Fe, Co) pairs ($N_{B\text{-}(Fe,Co)}$) and ΔT_x in the Fe-Co-Nd-B alloys. The N values in Fe_3B prism and the typical $Fe_{80}B_{20}$ amorphous alloy [18] are also shown in this figure. It is noted that the $N_{B\text{-}(Fe,Co)}$ values for the $Fe_{71}Co_{10}Nd_3B_{16}$ and $Fe_{61}Co_{10}Nd_3B_{26}$ alloys are very similar to the values in these reference alloys, indicating that trigonal prism-like local ordering units of B-(Fe, Co) may exist. The atomic distance of Nd-Fe pair was fitted to be 0.301 to 0.304 nm (see Fig. 4). Considering the large atomic size mismatch of about 46 % between Fe (atomic radius; r = 0.125 nm) and Nd (r = 0.182 nm), Nd atoms might be located at the second neighboring positions from B in the similar way

as tetragonal $Nd_2Fe_{14}B$ crystal and connect the trigonal prism units of B-(Fe, Co) to form a random network of them. Although the prism-like structure was identified, no supercooled liquid region was observed in the $Fe_{71}Co_{10}Nd_3B_{16}$ alloy, implying that the network of the prisms is not strong enough to maintain during heating at the lower boron concentration. As for the alloys with higher boron contents (x=35 or 40), the trigonal

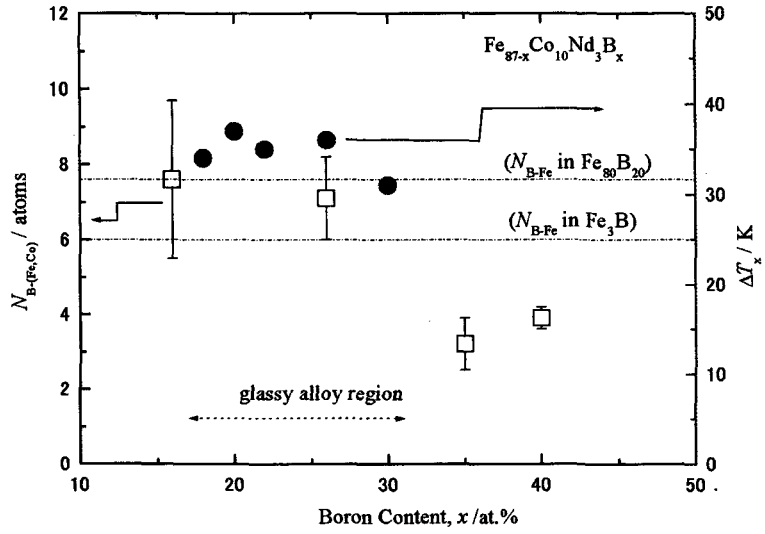

Fig.8 Coordination numbers of B-(Fe,Co) pairs, $N_{B\text{-}(Fe,Co)}$ (open square) and ΔT_x (full circle) in $Fe_{87-x}Co_{10}Nd_3B_x$ (x=16, 26, 35 or 40) glassy alloys. The values of $N_{B\text{-}Fe}$ in $Fe_{80}B_{20}$ and Fe_3B are also indicated for comparison.

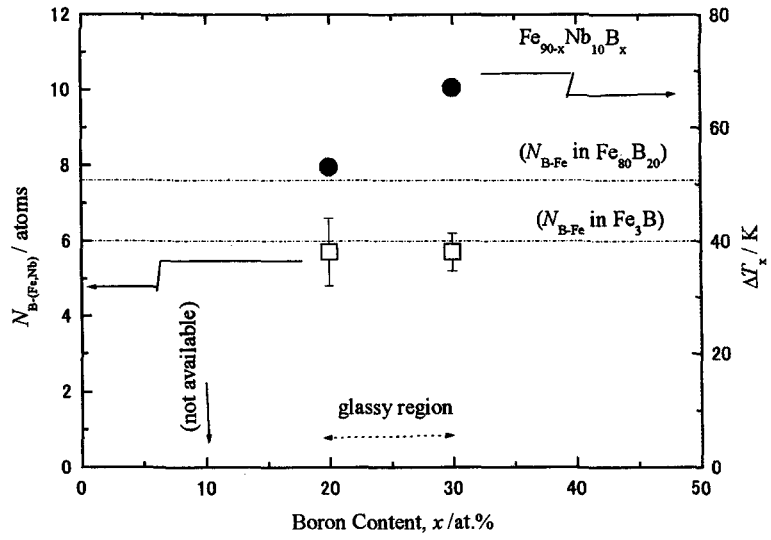

Fig.9 Coordination numbers of B-Fe pairs, $N_{B\text{-}Fe}$ (open square) and ΔT_x (full circle) in $Fe_{90-x}Nb_{10}B_x$ (x=10, 20 or 30) glassy alloys. The values of $N_{B\text{-}Fe}$ in $Fe_{80}B_{20}$ and Fe_3B are also indicated for comparison.

prism-like local structure is no longer dominant because the average $N_{B\text{-}(Fe,Co)}$ values are much smaller than those in the reference alloys.

Figure 9 shows the variation of $N_{B\text{-}(Fe,Nb)}$ in the Fe-Nb-B alloys. We can see from this figure that the coordination number around boron is nearly 6 in the glassy alloy region, suggesting that the local atomic unit in these alloys is similar to the trigonal prism of B-(Fe, Nb), in which Nb atom substitutes for Fe at the vertex site of the prism.

The prism should be somewhat distorted because of the rather large atomic size mismatch of about 18 % between Fe and Nb atoms. This feature has been identified in various Fe-M-B (M=transition metal) glassy alloys [19]. In the case of $Fe_{80}Nb_{10}B_{10}$ alloy, it is hard to distinguish the chemical short range ordered structure around boron.

The significant atomic size mismatches between the constituents and the large chemical affinities of Nd-B (ΔH_{mix}= -34 kJ/mol) pair in (Fe, Co)-Nd-B alloy or Nb-B (ΔH_{mix}= -39 kJ/mol) and Nb-Fe (ΔH_{mix}= -16 kJ/mol) pairs in Fe-Nb-B alloy may contribute to the strengthening of the network of the prisms, leading to the difficulty of rearrangements of the constituent elements on a long-range scale in these alloys.

4. Conclusions

The essential structural feature of the (Fe, Co)-Nd-B and Fe-Nb-B glassy alloys in the composition range exhibiting supercooled liquid region was characterized as the formation of the distorted dense random network of trigonal prism-like local units around boron connected with inserted Nd or substituted Nb. The significant difference in atomic sizes between the constituents and the strong chemical affinities of Nd-B or Nb-B and Nb-Fe pairs contribute to the strengthening of the network of the prisms, leading to the suppression of the rearrangement of the constituent elements on a long-range scale in these alloys.

Acknowledgements

The authors would like to thank Professors E. Matsubara and Y. Waseda of Tohoku University and Professor M. Nomura of Photon Factory of the National Laboratory for High Energy Accelerator Research Organization for their kind help on the AXS experiments and useful discussion.

REFERENCES

[1] A.Inoue, T.Zhang, T.Itoi and A.Takeuchi: Mater. Trans. JIM, **38**, 359 (1997).
[2] A.Inoue, T.Zhang and A.Takeuchi: Appl. Phys. Lett., **71**, 464 (1997).
[3] A.Inoue: Mater. Sci. Forum, **179-181**, 691(1995).
[4] A.Inoue: Sci. Rep. Res. Inst. Tohoku Univ., **A 42**, 1 (1996).
[5] A.Inoue: Mater. Trans. JIM, **36**, 866 (1995).
[6] W.Zhang and A.Inoue: Mater. Trans. JIM, **40**, 78 (1999).
[7] W.Zhang, K.Fujita, K.Fujita and A.Inoue: Mater. Trans. JIM, **40**, 1123 (1999).
[8] W.Zhang, M.Matsushita and A.Inoue: Mater. Trans. JIM, **41**, 1482 (2000).
[9] M.Imafuku, K.Yaoita, S.Sato, W.Zhang and A.Inoue: Mater. Trans. JIM, **40**, 1144 (1999).
[10] E.Matsubara, S.Sato, M.Imafuku, T.Nakamura, H.Koshiba, A.Inoue and Y.Waseda: Mater. Sci. & Eng., **A 312**, 136 (2001).
[11] K.Shirakawa, Y.Waseda and T.Masumoto: Sci. Rep. Res. Inst. Tohoku Univ., **A 29**, 229 (1981).
[12] Y.Waseda: *The Structure of Non-Crystalline Materials*, MacGraw-Hill, New York, (1980), pp.27-51 and pp.87-132.
[13] A.H.Narten and H.A.Levy: Science, **165**, 447 (1969).
[14] A.H.Narten: J. Chem. Phys., **56**, 1905 (1972).
[15] C.Park, M.Saito, A.Takeuchi, A.Inoue and Y.Waseda: High Temp. Mater. & Processing, **16**, 57 (1997).
[16] Y.Waseda and H.S.Chen: Sci. Rep. Res. Inst. Tohoku Univ., **A 28**, 143(1981).
[17] P.H.Gaskell: J. Non-Cryst. Solids, **75**, 329 (1985).
[18] T.Fujiwara, H.S.Chen and Y.Waseda: Z. Naturforsch **A 37**, 611(1982).
[19] M.Imafuku, S.Sato, T.Nakamura, H.Koshiba, E.Matsubara and A.Inoue: Mat. Res. Symp. Proc. Vol.**644**, (2001) L1.6.1.

(Received December 21, 2001; Accepted January 24, 2002)